

# THE EFFECTS OF STARTING CONDITION ON THE AGING

## RESPONSE OF AS-FORGED ALLOY 718

J.L. Burger\*, R.R. Biederman\*, and W.H. Couts\*\*

\*Materials Science and Engineering  
Mechanical Engineering Department  
Worcester Polytechnic Institute, Worcester, MA

and  
\*\*Research and Development Division  
Wyman Gordon Company, Millbury, MA

### ABSTRACT

The effects of four starting conditions on the isothermal aging response of as-forged Alloy 718 have been examined. As-forged Alloy 718 material was solution heat treated at either 1800F (982C) or 1950F (1066C) for 1 hour and quenched to room temperature. Samples from each solutionized condition were cold worked producing four starting conditions prior to aging. The samples from the four starting conditions were then isothermally aged at 1800F (982C), 1650F (899C), 1500F (816C), and 1200F (648C) for various lengths of time and subsequently quenched to room temperature. Microstructural analysis was performed to correlate structural changes to hardness data.

The  $\delta$  morphology generated during isothermal aging at 1800F (982C) depends on the prior microstructure condition. The 1950F (1066C) solution condition when aged at 1800F (982C) resulted in the formation of  $\delta$  in a plate morphology. The 1800F (982C) solution condition started with platelet  $\delta$  which spheroidizes with added time. Cold working of both prior to aging at 1800F (982C) distributes the  $\delta$  more uniformly throughout the microstructure and produces a more uniform  $\delta$  size distribution. Isothermally heat treating at 1650F (899C) precipitated  $\delta$ ,  $\gamma'$ , and  $\gamma''$  nearly simultaneously yielding only a minor hardening response on subsequent aging. Both  $\gamma'$  and  $\gamma''$  were observed in the 1650F (899C) and 1500F (816C) aging groups. Either  $\gamma''$  nucleated initially or both  $\gamma''$  and  $\gamma'$  formed simultaneously. In this study,  $\gamma'$  was never observed to form prior to  $\gamma''$ . Solution temperature does not appear to have a significant effect on the precipitation growth kinetics of  $\gamma'$  or  $\gamma''$ , however, cold working promotes nucleation of both. Nucleation and growth of  $\delta$  triggers the dissolution of the metastable  $\gamma''$  phase which serves as the Niobium feeding source for further  $\delta$  growth. The 1800F (982C) starting condition contained a substantial amount of  $\delta$  which ties up much of the available Niobium in the alloy, limiting the amount of  $\gamma''$  that can form. As the amount of  $\delta$  increases, the hardness of the alloy decreases due to decreasing amounts of  $\gamma''$ .

## Introduction

The steam and gas turbine industry has great interest in forgings made from Alloy 718 because of its high strength, ductility, and weldability (1,2,3). Commonly an ingot is forged to its desired shape at an elevated temperature, solution treated, and aged to produce the desired microstructure and properties. The forging can be either solution heat treated followed by water quenching with subsequent aging or forged, quenched and direct aged. Maintaining a uniform stable microstructure throughout a large forging is a difficult task with this alloy (1,4). Often the final forging will vary in section size (i.e. thickness) and contains different amounts of deformation throughout. The microstructure can be expected to vary from region to region in the forging, resulting in nonuniform mechanical properties (4).

The objective of this study is to develop an understanding of the dynamic aging response of forged Alloy 718 under different solutionizing and working conditions prior to aging. This investigation will only be concerned with  $\delta$ ,  $\gamma''$ , and  $\gamma'$  isothermal transformation kinetics from annealed and moderately cold worked starting material.

## Experimental Procedure

As-forged Alloy 718 material was solution heat treated, quenched to room temperature, and either aged directly or cold worked 20% and then aged. The cold work was achieved by swaging at room temperature which provided a uniform working condition throughout the cross-section of the rods. The following notation will be used to reference these starting conditions: CONDITION A - Solutionized at 1950F (1066C), CONDITION B - Solutionized at 1800F (982C), CONDITION C - Solutionized at 1950F (1066C) and Cold Worked, and CONDITION D - Solutionized at 1800F (982C) and Cold Worked. The aging temperatures chosen for this study are 1200F (648C), 1500F (760C), 1650F (899C), and 1800F (982C). There are few Time-Temperature Transformation (TTT) diagrams in existence for Alloy 718. Eiselstein (5) and Superalloys II (14) published diagrams which served as the initial basis for choosing the aging temperatures and times used for this investigation. Aging at 1200F (648C) was performed in a conventional furnace while the remaining samples were aged in a fluidized bed. The fluidized bed provided quick heat-up times and tight temperature control at elevated temperatures and proved to be a necessary heat treating medium for this study. The samples were removed from the respective heat treating media and quenched to room temperature in water every 2<sup>h</sup> minutes (n = 0 to 12).

Hardness measurements were taken and microstructural analysis was performed to correlate these data to microstructural changes occurring during aging. All the samples were electrolytically polished with a 10% HCl-methanol solution for optical and Scanning Electron Microscopy (SEM) observation. To document the presence of  $\delta$  or Laves phases an extraction process using a HCl-methanol electrolyte was performed. Xray diffraction and SEM observation of these extractions allowed the phases present, morphologies, and chemistries to be identified with respect to the representative microstructures.

Thin foil Transmission Electron Microscopy (TEM) analysis was performed on selected samples to observe  $\gamma'$  and  $\gamma''$  nucleation, growth, and stability during aging. The  $[100]\gamma$  zone was used to observe these precipitates. By dark field imaging a (010) type reflection of the  $[100]\gamma$  zone, the  $\gamma''$  and  $\gamma'$  can be distinguished from each other (6,7). This superlattice reflection represents one of the  $\gamma''$  orientations and all of the  $\gamma'$  present. Any confusion between  $\gamma'$  and the  $[001]\gamma''$  orientation can be eliminated by dark field imaging this type of reflection.

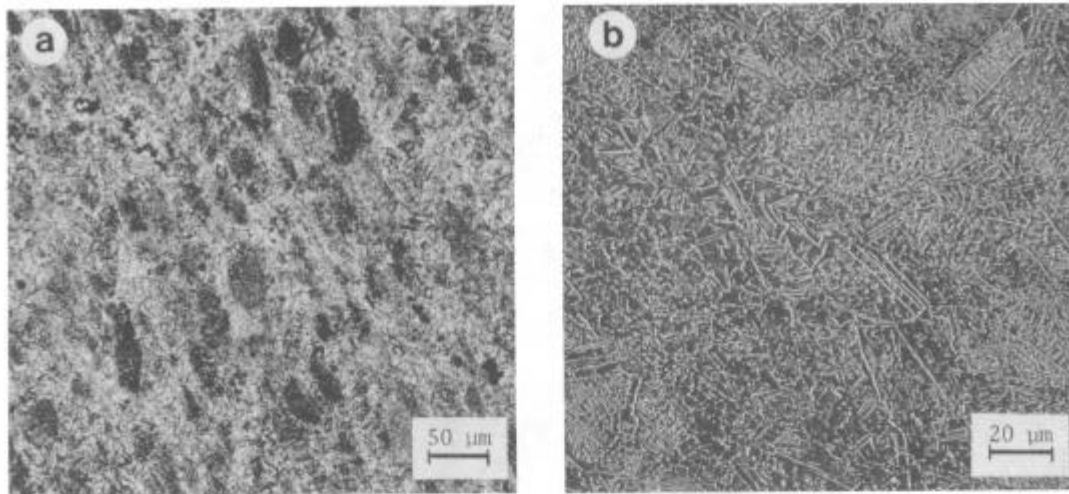


FIGURE 1 - Microstructure of Alloy 718 Forged @ 1825F (996) Air Cooled  
a.) Optical b.) SEM

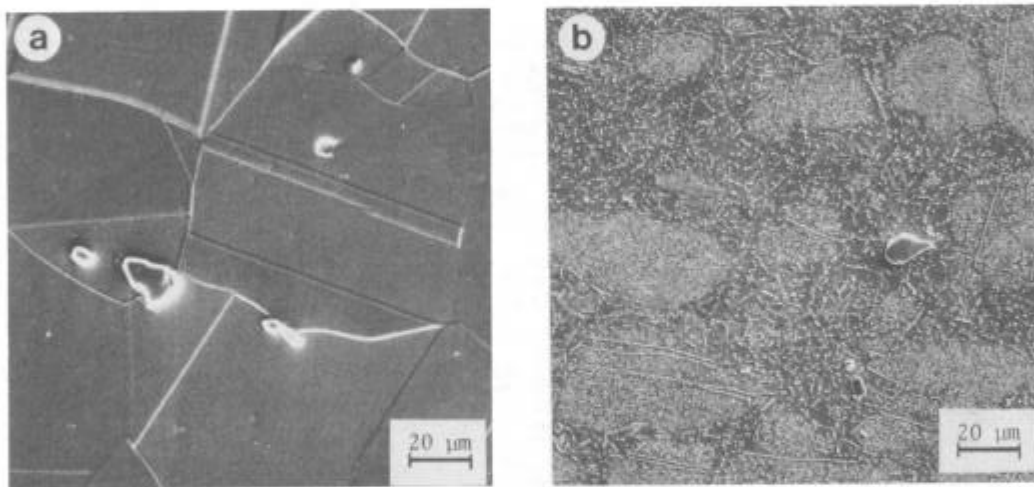


FIGURE 2 - Microstructure of Forged Alloy 718 after Solutionizing  
a.) Condition A b.) Condition B

### Results and Discussion

#### Microstructural Evaluations of Starting Conditions

The microstructure of as-forged Alloy 718 material is shown in Figure 1. This material was forged from a furnace at 1825F (996C) and air cooled. The structure contains a fine but mixed grain size with a large volume fraction of  $\delta$ .

Figure 2 illustrates the microstructure of Condition A. This solution treatment is a  $\delta$ ,  $\gamma'$ , and  $\gamma''$  solution anneal but large carbides are still evident. Notice that this solution treatment yields a large uniform fully recrystallized grain structure. In essence, all the elements are in solution except minor amounts of Nb, Ti, Mo and C which are tied-up in MC carbides.

Thin foil TEM analysis found planar type dislocations in Condition A. These dislocations were produced by quenching from the solution temperature and are consistent with findings by Hassett (8) and Cowie (9) in another superalloy. SAD analysis of the matrix verified the solution treatment of  $\gamma'$  and  $\gamma''$ . The microstructure representing Condition B is also shown in Figure 2. The grain size is much smaller than achieved in Condition A and a large volume fraction of  $\delta$  is observed. Grain boundaries are less distinct because of the large amount of  $\delta$ . TEM observation found Condition B to consist of a partially recrystallized microstructure with the recrystallized regions containing spheroidized  $\delta$  and the unrecrystallized regions containing platelet  $\delta$ .

### Hardness Measurements

Upon completion of heat treating, hardness measurements were taken. The aging response hardness data for each starting condition are shown in Figure 3. As can be seen, each starting condition has a different initial hardness value but a similar aging response for each temperature. The starting hardness values ( $R_c$ ) for the aging study were: Condition A (7), Condition B (28), Condition C (30), and Condition D (35).

Condition A consisted primarily of a recrystallized solid solution ( $\gamma$ ) with a uniform coarse grain size. A homogeneous distribution of the elements, necessary for coherent precipitation (i.e. Nb, Ti, and Al), produced the classical age hardening response for this starting condition. Cold working this starting condition work hardened the material to 30  $R_c$  and also accelerated nucleation of the strengthening phases slightly.

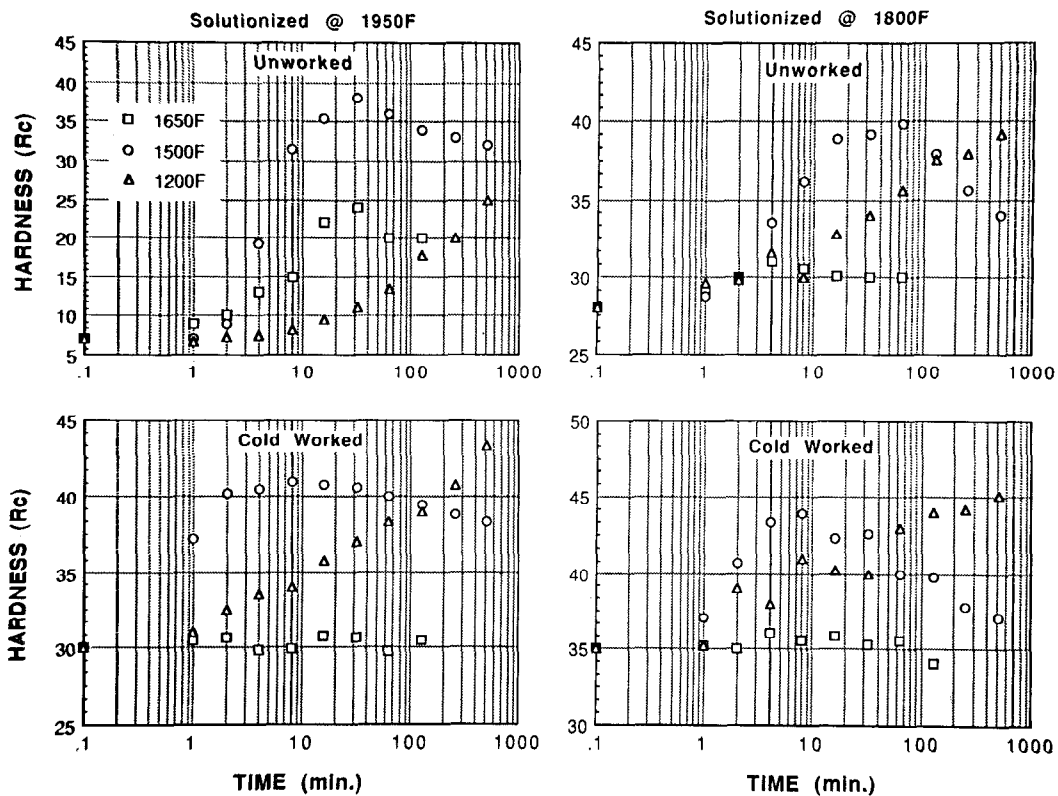


FIGURE 3 - Hardness Data of Each Starting Condition Upon Aging

Condition B had a starting hardness value of 28  $R_c$  due to partial recrystallization and large  $\delta$  volume fraction. Aging this starting condition yielded a lower net age hardening effect due to the lower availability of Nb in solution since much of it is tied up in  $\delta$ . Cold working this starting condition accelerated the age hardening slightly as well as added complexity to the hardening response.

Assuming diffusion to be the rate controlling mechanism for the precipitation of  $\gamma''$  in  $\gamma$ , hardness data in Figure 4 for Condition A can be used to estimate the activation energies for the diffusion of Nb in  $\gamma$  by using the time required to reach a given hardness for all three aging temperatures. The hardness values used are  $R_c$  of 10, 15, and 20. The activation energies (Q) estimated for these values are 13.4, 14.7, and 16.7 kcal/mole, respectively. Muramatsu et.al. (12) calculated Q for the diffusion of Nb in two ordered phases, NiNb and Ni<sub>3</sub>Nb. These values were 39 and 17 kcal/mole, respectively. The Diffusion Data Center at the Metallurgy Division of the National Bureau of Standards has stated that they could not find data for the diffusion of Niobium at lower concentration levels in Ni rich solid solutions.

#### Microstructural Characterization Aging Condition A (High Temperature Solutionize)

Aging at 1800F (982C). Isothermally aging at this temperature should yield  $\delta$  and possibly Laves formation. To identify which phases were present, an extraction using an HCl-methanol electrolyte was taken of a sample aged for over 64 hours. Xray diffraction data for this extraction versus published data (13) support the presence of  $\delta$  and NbC but no Laves was found. The  $\delta$  platelets were observed to nucleate at grain and twin boundaries and grow according to their crystallographic relationship with the matrix.  $\delta$  is first observed at 8 minutes for this starting condition.

Aging at 1650F (899C). According to published TTT diagrams, aging at this temperature would precipitate  $\gamma''$  and  $\delta$  at nearly the same time. From the aging curve a hardness increase is observed but the hardness only reaches 22  $R_c$  before decreasing slightly.  $\delta$  precipitation at grain and twin boundaries is observed with some intragranular formation. Nonhomogeneous nucleation and rapid coarsening of  $\gamma''$  precipitates are observed and frequently particles are oriented in arrays along some [110] type direction. The  $\gamma''$  precipitates are believed to be aligned in this fashion by forming on dislocations produced by quenching from solution treatment.

Aging at 1500F (816C). Aging at this temperature precipitated  $\gamma'$ ,  $\gamma''$ , and  $\delta$ . Looking at the aging curve for this starting condition, the alloy hardness peaks at  $R_c$  40 at approximately 1.5 hours. Observing a sample aged for 2 hours and 8 minutes (Figure 4) indicates  $\delta$  precipitation at grain boundaries and a uniform distribution of intragranular  $\gamma'$  and  $\gamma''$ . To observe both  $\gamma'$  and  $\gamma''$  precipitates, the [100] SAD pattern was generated. The bright field/dark field pair of the (010) reflection allows for proper identification. One  $\gamma''$  orientation and all the  $\gamma'$  particles are observed in dark field. The  $\gamma'$  particles are not as pronounced in dark field as are  $\gamma''$  precipitates. Note that  $\gamma''$  and  $\gamma'$  precipitates are observed as separate and duplex particles. This would indicate a close relationship between their nucleation and growth behavior. The spherical  $\gamma'$  precipitates are approximately 500 Å in diameter while the  $\gamma''$  disks are 150 Å in the c dimension and 800 Å in diameter. A depletion of precipitates is observed surrounding grain boundary and intragranular  $\delta$ . This observation illustrates the stability preference of  $\delta$  over  $\gamma''$ . The grain boundary  $\delta$  precipitates nucleate at the boundary and grow into the matrix according to their crystallographic relationship. The intragranular formation of  $\delta$  nuclei is

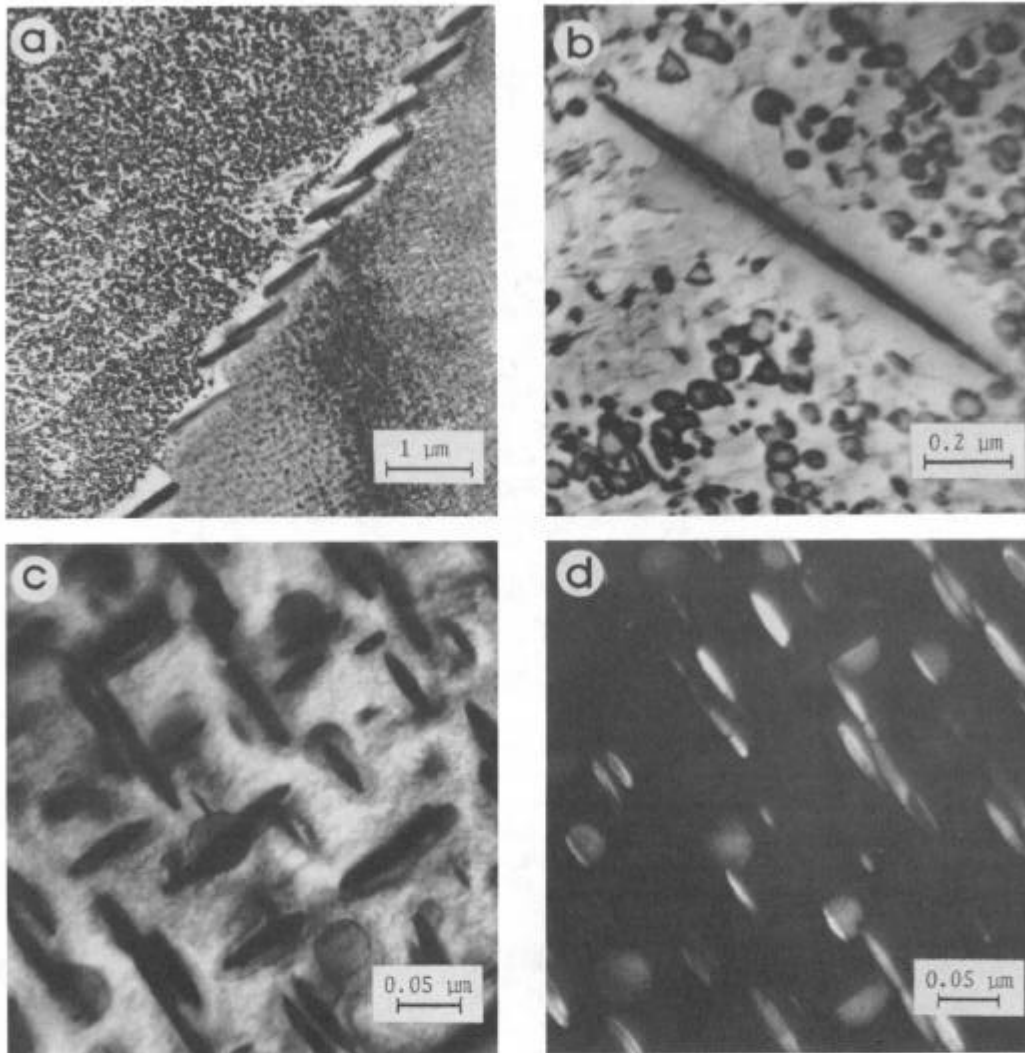


FIGURE 4 - Condition A Aged for 2 hrs. 8 min. @ 1500F (816C)  
 a.) Grain Boundary  $\delta$  b.) Intragranular  $\delta$   
 c & d.) Bright and Dark Field Images of  $\gamma'$  and  $\gamma''$

thought to be due to stacking faults in  $\gamma''$  produced by rapid  $\gamma''$  growth and high coherency strains (10,11). As time progresses  $\gamma''$  dissolves in order to feed the more stable  $\delta$  phase. Figure 5 illustrates the microstructure of a sample aged for 64 hours and 16 minutes. Large  $\delta$  needles and intragranular  $\gamma''$  are observed. An interesting observation in the TEM micrograph is the presence of  $\gamma'$  between the  $\delta$  needles.  $\gamma'$  is therefore more stable than  $\gamma''$  at this temperature and time and remains following  $\gamma''$  dissolution and subsequent  $\delta$  formation.

At shorter aging times, one can not determine the time at which precipitation begins through mere observation. Because of this, the  $\gamma'/\gamma''$  start times will be defined through SAD patterns. Figure 6 contains [100] SAD patterns for samples aged for 2 and 4 minutes. The appearance of superlattice reflections after 4 minutes indicates that  $\gamma''$  has formed or that both  $\gamma'$  and  $\gamma''$  have formed. Tiny particles can be seen in the bright field image by coherency strain fields which surround them. The  $\gamma''$  precipitates are approximately 40 Å (5-10 unit cells) thick in the c direction. Dark field imaging these precipitates was difficult due to the low intensity of the superlattice reflections and size of these precipitates. The nucleation

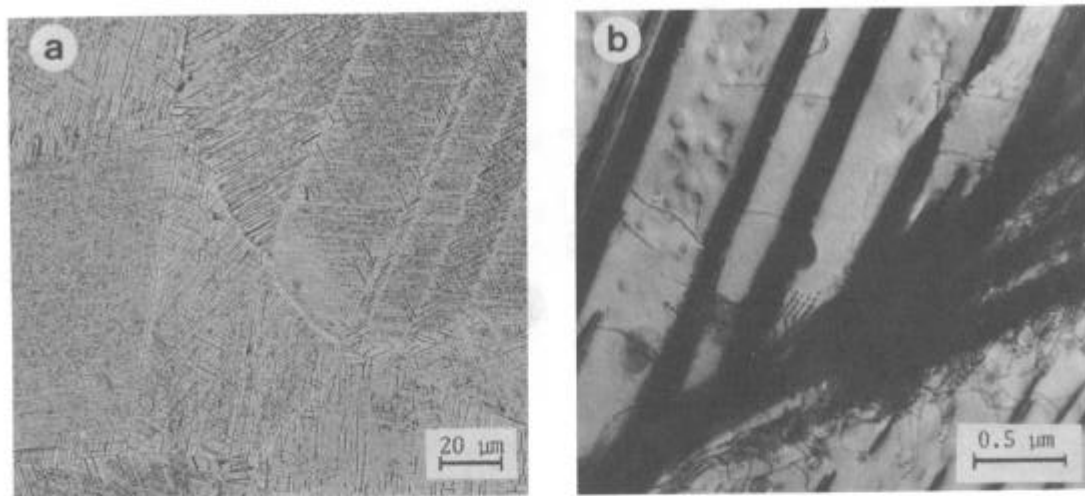


FIGURE 5 - Microstructure of Condition A Aged @ 1500F (816C) for 64 hrs. 16 min.; a.) Optical b.) SEM

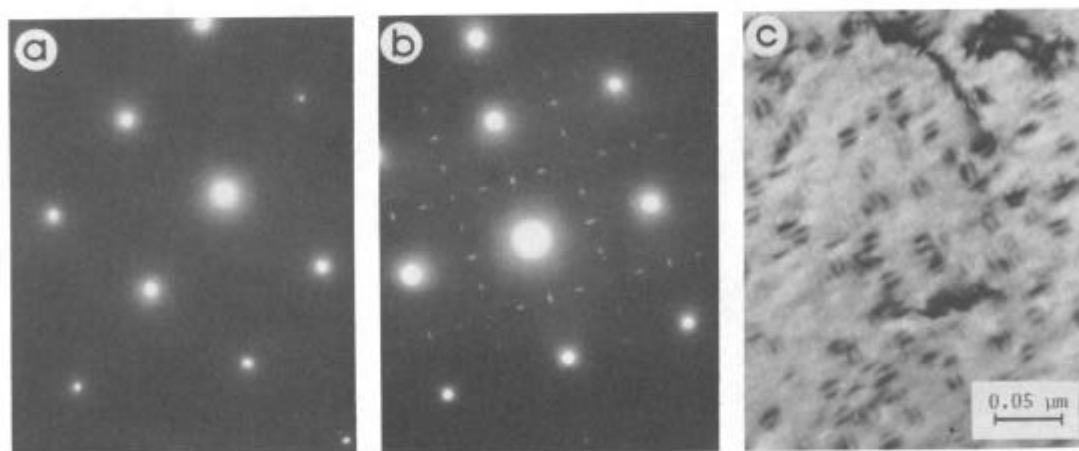


FIGURE 6 - [100] $\gamma$  SAD Patterns and Bright Field Image of Early  $\gamma'$ / $\gamma''$  Precipitation in Condition A Aged @ 1500F (816C)  
a.) 2 minutes b.) 4 minutes c.) Bright Field after 4 minutes

of these particles is quite uniform as well as their size at longer times. This would indicate that the increase in hardness as a function of time is primarily due to coarsening of these particles and hence the coherency strains. It should be noted that either  $\gamma''$  formed first or both  $\gamma'$  and  $\gamma''$  precipitated nearly simultaneously.  $\gamma'$  was never observed to form before  $\gamma''$ .

Aging at 1200F (648C). The aging curve for this temperature illustrates the precipitation sluggishness of  $\gamma'$  and  $\gamma''$ . There is little evidence of coherent precipitation up to 1 hour. A sample aged for 136 hours examined by SEM and TEM found  $\gamma''$  precipitates that were approximately 200Å in diameter and 50Å thick. At the shorter aging times, where hardening is evident (at 64 minutes), the classical [100] SAD pattern was obtained. Low intensity of the superlattice reflections made it difficult to image  $\gamma'$  or  $\gamma''$ . It can be noted however, that  $\gamma''$  or both  $\gamma'$  and  $\gamma''$  are evident at the earliest stages of precipitation for this aging temperature regardless of starting condition.



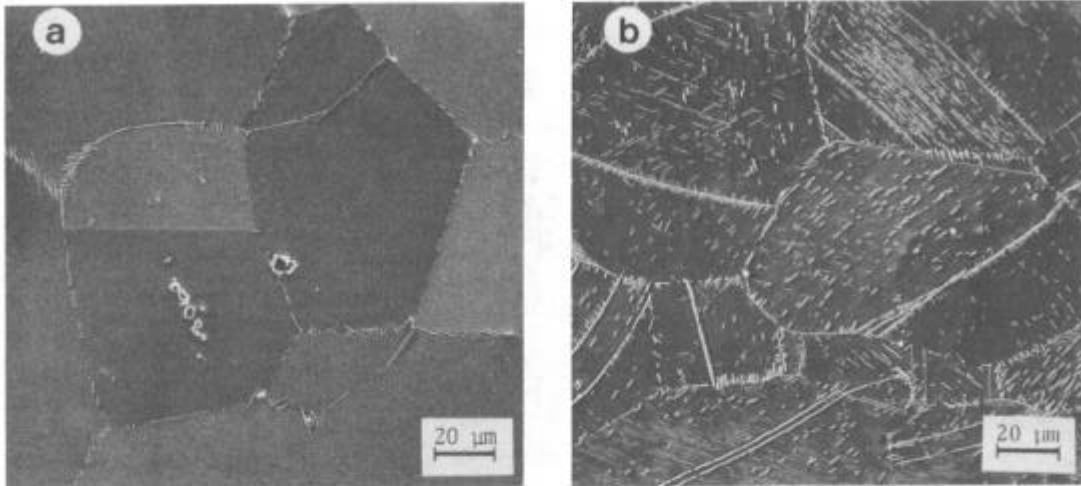


FIGURE 7 - Aging Condition A (a) and Condition C (b) for 17 hrs. 4 min. @ 1500F (816C)

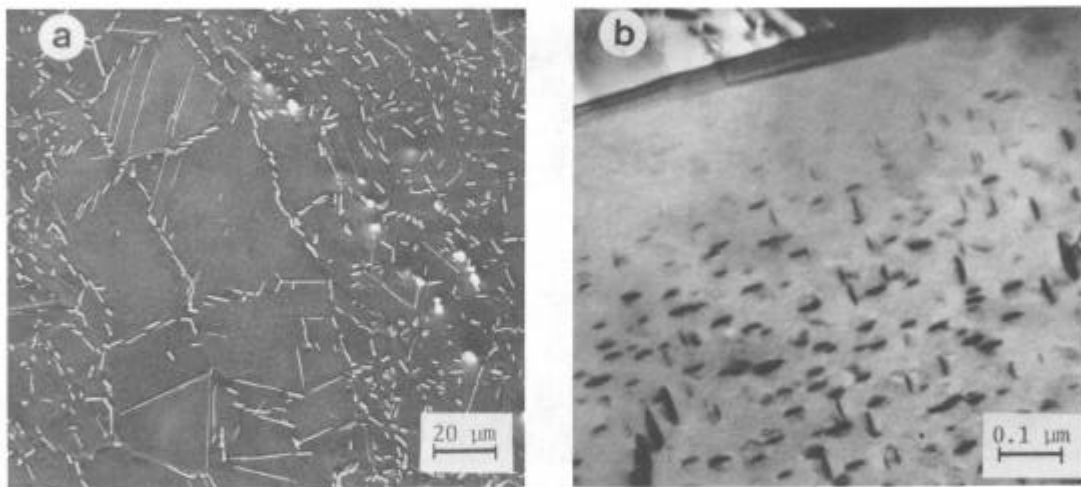


FIGURE 8 - Condition B Aged for 2 hrs. 8 min. @ 1500F (816C)  
a.) SEM b.) TEM

Aging Condition C (High Temperature Solutionize and Cold Work)

Aging at 1800F (982F). Heat treating the cold worked material in the fluidized bed at this temperature permitted recrystallization to occur followed by  $\delta$  formation. Hardness data and microstructural analysis indicated that recrystallization started after 1 minute and was complete by 4 minutes. Further aging at this temperature resulted in  $\delta$  precipitation only at prior grain boundaries.

Aging at 1650F (899C). Cold working seemed to have an effect on hardening as seen by the aging curve for this starting condition. The hardness increase due to coherent precipitation at this temperature was negligible. Recrystallization was not observed even after 2 hours. For samples aged for 2 hrs. and 8 min. the volume fraction of  $\delta$  is higher and more uniform in the cold worked sample than the unworked. The dispersion of incoherent  $\delta$ , nonuniform  $\gamma''$  nucleation, and rapid  $\gamma''$  growth are responsible for the lack of hardening as time progresses.



Aging at 1500F (816C). Aging this starting condition at 1500° F (816° C) produced similar results as those observed in the unworked condition. The aging curve for this starting condition demonstrates a hardening response which starts at 30 R<sub>C</sub> and peaks at 40 R<sub>C</sub>. The work hardening produced by cold working yields a start hardness of 30 R<sub>C</sub>. The net hardening effect due to coherent precipitation is 10 R<sub>C</sub> as opposed to 30 R<sub>C</sub> for the unworked starting condition. The classical [100] SAD pattern was obtained after 1 minute which indicates that precipitation of  $\gamma''$  or both hardening phases occurred before 1 minute at this temperature. As described earlier, this SAD pattern for the unworked condition was observed in the 4 minute sample. Samples from Conditions A and C aged for 17 hours and 4 minutes are shown in Figure 7. These SEM micrographs illustrate the  $\delta$  distribution difference for the cold worked and unworked starting conditions.

Aging Conditions B and D (Low Temp. Solutionize With & Without Cold Work)

Aging at 1800F (982C). Heat treating Condition B at this temperature allowed the as-forged (warm worked) structure to fully recrystallize. Along with recrystallization, the existing  $\delta$  suppresses grain growth and spheroidizes with time. Condition D heat treated at this temperature fully recrystallized in 4 minutes; following a similar time frame as Condition C.

Aging at 1650F (899C) Conditions B and D had similar aging responses at this temperature according to their aging curves. A negligible hardening effect was observed. Each microstructure started with a significant  $\delta$  volume fraction (30%) which limits the  $\gamma''$  precipitation behavior by tying up Nb. As discussed earlier for Condition A, the precipitation of  $\gamma''$  at this temperature was not uniform and the net hardening effect was only 15 R<sub>C</sub>.  $\delta$  is decorating nearly all the boundaries and also intragranularly as a blocky, slightly spheroidized morphology. The recrystallized regions which have a more random distribution of  $\delta$  are lacking the strengthening precipitates. The existing  $\delta$  seems to not only tie-up the Nb but also accommodate  $\delta$  growth easier than that seen in Condition A. This is seen by observing the depletion zone surrounding  $\delta$ . Cold working permits more intragranular  $\delta$  formation by nucleation on dislocations than the unworked condition but this type of precipitation is limited.

Aging at 1500F (816C). The aging curves for this temperature indicate significant hardening for Conditions B and D. Condition B demonstrated a net hardening effect of 10 R<sub>C</sub>. Compared to Condition A, the net effect was much less. This is due to the unavailability of Nb for  $\gamma''$  growth. Thin foil SAD analysis showed the same nucleation time frame (4 minutes) for  $\gamma'$  and  $\gamma''$  with the distribution being dependent on the amount of surrounding  $\delta$ . In Figure 8 SEM and TEM micrographs are shown for Condition B aged for 2 hours and 8 minutes. The SEM micrograph shows the  $\delta$  distribution with some large grain regions which are unrecrystallized from the solution treatment. A typical grain boundary of the finer grained regions is shown in the TEM micrograph. A fine dispersion of both  $\gamma'$  and  $\gamma''$  is evident with a depletion zone along the boundary. When  $\delta$  formation starts,  $\gamma''$  near the boundaries dissolves and Nb apparently diffuses along the grain boundaries to a nearby  $\delta$  particle where it is consumed.  $\delta$  growth with time is supported by this grain boundary piping mechanism. Limited nucleation of new  $\delta$  was noticed. Condition D yielded a  $\gamma'/\gamma''$  nucleation time of <1 minute and the same net hardening effect as the solutionized condition. Looking at the longer aging times, a more random distribution of  $\delta$  was found.

## Conclusions

The objective for this study was to document the effect of material starting condition on the precipitation behavior of Inconel 718 during isothermal aging. This investigation focused on the two coherent phases ( $\gamma'$  and  $\gamma''$ ) and the incoherent  $\delta$  phase. The following conclusions can be drawn from the documented results:

1. Conditions A and B produced different  $\delta$  morphologies when heat treating at 1800F (982C). Condition A precipitated  $\delta$  in a plate morphology which nucleated and grew along grain and twin boundaries. Condition B started with  $\delta$  in the microstructure and spherodized this phase with time. Cold working each of these conditions allowed both microstructures to fully recrystallize in 4 minutes. Condition C precipitated  $\delta$  at prior grain and twin boundaries while Condition D spherodized  $\delta$  with time.
2. Nonuniform nucleation and rapid growth of  $\gamma'$  and  $\gamma''$  along with simultaneous  $\delta$  formation accounts for the minor hardening response at 1650F (899C).
3.  $\gamma'$  and  $\gamma''$  were observed in the 1650F (899C) and 1500F (816C) aging groups. Either  $\gamma''$  or both  $\gamma'$  and  $\gamma''$  nucleate initially. Solutionizing condition does not appear to have an effect on their precipitation behavior. Cold working moves the  $\gamma'/\gamma''$  start line from 4 minutes to less than 1 minute.
4. Nucleation of  $\delta$  triggers the dissolution of the metastable  $\gamma''$  phase which serves as a feeding source for further  $\delta$  growth.  $\delta$  nucleates at grain and twin boundaries in the unworked state and more uniformly in the cold worked condition.
5.  $\gamma'$  remains after  $\gamma''$  has been totally consumed;  $\gamma'$  is not the precursor to  $\gamma''$ .
6. Condition B contained a substantial amount of  $\delta$  in the starting microstructure. The  $\delta$  altered the aging response by tying-up Nb which is needed by the strengthening  $\gamma''$  phase. When the  $\delta$  start line is crossed, the existing  $\delta$  particles trigger the dissolution process and consume available Nb in order to grow. As the amount of  $\delta$  increases, the strengthening of the alloy decreases due to decreasing amounts of  $\gamma''$ .
7.  $\delta$  appears to serve no useful purpose other than to limit grain growth of the  $\gamma$  phase during the solutionizing and aging treatments.

## REFERENCES

1. Irving, R.R., "Alloys 718: The Workhorse of the Superalloys", Iron Age, June 10, 1981.
2. Paulonis, D.F., Oblak J.M., and Duvall D.S., "Precipitation in Nickel-Base Alloy 718", Trans. of ASM, Vol. 62, 1969.
3. Wagner, H.J. and Hall, A.M., "Physical Metallurgy of Alloy 718", DMIC Report, Battelle Memorial Institute, Columbus, Ohio, 1965.
4. Radavich, J.F. and Coutts, W.H., Jr., "Factors Affecting Delta Phase Precipitation and Growth at Hot Worked Temperatures for Direct Aged INCO 718", Superalloys 84, Conf. Proc., 1984.
5. Eiselstein, H.L., "Metallurgy of a Columbium-Hardened Nickel-Chromium-Iron Alloy", ASTM Publication, 1965.
6. Oblak, J.M., Paulonis, D.F., and Duvall, D.S., "Coherency Strengthening in Ni Base Alloys Hardening by  $DO_{22}$  Precipitates", Met. Trans. Vol. 5, January, 1974.
7. Cozar, R., and Pineau, A., "Morphology of  $\gamma'$  and  $\gamma''$  Precipitates and Thermal Stability of Inconel 718 Type Alloys", Met. Trans., Vol. 4, Jan. 1973.
8. Hassett, D.F., "Effect of Thermomechanical Processing on the Dislocation Characteristics in Incoloy 901", M.S. Thesis, W.P.I., 1985.
9. Cowie, J., "A Study of the Dislocation Substructure in Press Forged Incoloy 901, Nickel Base Superalloy", M.S. Thesis, W.P.I., 1980.
10. Kirman, I., and Warrington, D.H., "The Precipitation of  $Ni_3Nb$  Phases in a Ni-Fe-Cr-Nb Alloy", Met. Trans., Vol. 1, Oct. 1970.
11. Sundararaman, M., Mukhopadhyay, P., and Banerjee, S., "Precipitation of the  $\delta$ - $Ni_3Nb$  Phase in Two Nickel Base Superalloys", Met. Trans., Vol. 19A, March, 1988.
12. Muramatsu, P., Roux, F., and Vignes, A., "The Influence of Pressure on the Formation of Intermetallics in Niobium/Nickel Diffusion Couples", Trans. of the Japanese Institute of Metals, 1975.
13. Donachie, M.J. and Kriege O.H., "Phase Extraction and Analysis in Superalloys", ASTM Report, 1972.
14. Brown, E.E., and Muzyka, D.R., "Nickel-Iron Alloys", Superalloys II, John Wiley and Sons, New York, 1987.